J Nanostruct 16(4): 5688-5701, Autumn 2026

RESEARCH PAPER

Studying the Efficacy of Nano-Silver Particles Produced from Pomegranate (Punica granatum) Peels Against Pseudomonas aruroginosa

Hadi Salman AL- Lami [1,2] *, *Rabab Qasim Mohammed AL-Segar* [1]

[1] *Shatt Al-Arab University College, Basra, Iraq*

[2] *College of Science, University of Basra, Basra, Iraq*

ARTICLE INFO

Article History:
Received 05 May 2026
Accepted 05 July 2026
Published 01 October 2026

Keywords:
Cytotoxicity
Nano-silver
Pseudomonas pomegranate
Punica granatum

ABSTRACT

Pseudomonas aeruginosa (*P. aeruginosa*) is a major opportunistic pathogen associated with hospitals, particularly in cases of burns and wounds, due to its high antibiotic resistance and biofilm formation capabilities. This study aimed to isolate and identify *P. aeruginosa* from various clinical samples, assess its antibiotic resistance, investigate the antibacterial and antibiofilm effects of silver nanoparticles (AgNPs), evaluate their synergistic activity with certain antibiotics, and investigate their cytotoxicity.Two hundred clinical samples were collected, and 58 confirmed isolates were obtained, representing an overall isolation rate of 29%. The isolates exhibited high resistance rates to several antibiotics, particularly piperacillin and ciprofloxacin. The results showed that silver nanoparticles produced from pomegranate (*Punica granatum*) peels demonstrated significant inhibitory activity against the tested isolates and the ability to reduce and eliminate biofilm formation at specific concentrations. Synergistic testing using the checkerboard method and a decrease in the FICI value confirmed a synergistic effect between the AgNPs and some antibiotics. The time-kill test also showed a significant decrease in the number of colony-forming units. Cytotoxicity testing (MTT) on human fibroblasts indicated an acceptable safety margin at effective concentrations. The results indicate that silver nanoparticles may represent a promising adjunctive therapy option in combating multi-resistant *P. aeruginosa* infections, particularly those associated with biofilm formation, with the need for further studies to enhance their clinical application.

How to cite this article
AL- Lami H., AL-Segar R . Studying the Efficacy of Nano-Silver Particles Produced from Pomegranate (Punica granatum) Peels Against Pseudomonas aruroginosa. J Nanostruct, 2026; 16(4):5688-5701. DOI: 10.22052/JNS.2026.04.098

INTRODUCTION

Pseudomonas aeruginosa (*P. aeruginosa*) is a major opportunistic Gram-negative bacterium associated with hospital-acquired infections, particularly in immunocompromised patients, burn patients, intensive care patients, and cystic fibrosis patients. This bacterium is characterized by its high adaptability to the environment, its production of multiple virulence factors, and its natural and acquired resistance to a large number of antibiotics. In recent years, there has been an increasing number of global reports of multidrug-resistant (MDR) and extensively resistant (XDR) strains, leading to fewer treatment options and higher morbidity and mortality rates [1, 2]. The

* *Corresponding Author Email: dr.hadi.salman@sa-uc.edu.iq*

This work is licensed under the Creative Commons Attribution 4.0 International License.
To view a copy of this license, visit http://creativecommons.org/licenses/by/4.0/.

danger posed by *P. aeruginosa* is also attributed to its remarkable ability to form biofilms, which are organized bacterial communities surrounded by an extracellular matrix that protects cells from the effects of environmental factors, antibiotics, and the immune system [3]. These biofilms act as a physical and chemical barrier that impedes antibiotic penetration and induces physiological changes within the bacterial cells that reduce their sensitivity to treatment [4]. Therefore, conventional treatments often fail to completely eradicate biofilm-associated infections, leading to persistent inflammation and chronic relapses. In light of these challenges, nanotechnology has emerged as a promising avenue for developing antimicrobial agents with multiple mechanisms of action. Silver nanoparticles (AgNPs) are among the most studied nanomaterials due to their broad spectrum of antibacterial, antifungal, and antiviral activity [5]. The mechanism of action of silver nanoparticles relies on several simultaneous pathways, including disrupting cell membrane integrity, increasing reactive oxygen species (ROS) production, binding to proteins containing sulfhydryl groups, and inhibiting DNA replication [6]. The multiplicity of these mechanisms reduces the likelihood of rapid resistance development compared to conventional antibiotics, making them a potential therapeutic option against resistant strains, including P. aeruginosa (7). Despite the effectiveness of chemically synthesized nanoparticles, traditional methods for their preparation may require toxic chemicals and high-energy conditions, raising environmental and health concerns. Therefore, recent research has focused on the biosynthesis, or "green," of nanoparticles using plant extracts, due to their environmental safety, low cost, and ease of application [8]. This method relies on the presence of phenolic compounds, flavonoids, tannins, and other secondary compounds in plants, which act as reducing agents and stabilizers for silver ions, leading to the formation of stable and bioavailable nanoparticles. *Punica granatum* (pomegranate) is a plant rich in bioactive compounds and is widely cultivated in the Middle East, including Iraq. Pomegranate peels constitute a significant portion of the fruit's total mass and are often discarded as agricultural waste. However, these peels contain high concentrations of ellagitannins, punicalagin, gallic acid, and flavonoids, compounds known for their antioxidant and antimicrobial properties [9]. Utilizing pomegranate peels in the green synthesis of silver nanoparticles represents a sustainable model that combines reducing agricultural waste with developing innovative therapeutic materials. Recent studies have shown that silver nanoparticles synthesized using pomegranate peel extract possess antibacterial activity that sometimes surpasses that of the crude plant extract alone [10]. This is attributed to the synergy between silver ions and phenolic compounds, where this interaction leads to increased bacterial membrane permeability, induction of intracellular oxidative stress, and disruption of biofilm formation [11]. Furthermore, some evidence suggests that nanoparticles prepared using green methods may exhibit higher biocompatibility and lower cytotoxicity compared to their chemically synthesized counterparts, enhancing their potential for use in medical applications [12, 13]. Investigating the effect of silver nanoparticles extracted from pomegranate peels on *P. aeruginosa* is of particular scientific importance given the increasing prevalence of resistant strains, especially in clinical settings with a high infection burden. Assessing anti-biofilm activity is also crucial, as biofilm plays a critical role in infection persistence. Furthermore, the physicochemical properties of nanoparticles—such as size, shape, surface charge (zeta potential), and stability—are pivotal in determining their biological efficacy, with efficacy typically increasing with smaller size and a higher surface area-to-volume ratio. Based on the foregoing, employing green synthesis technology for silver nanoparticles using pomegranate peels represents a promising strategy that combines environmental sustainability with advanced medical applications. Accordingly, this study aims to evaluate the antibacterial and anti-biofilm effects of silver nanoparticles synthesized from pomegranate peels against *P. aeruginosa*, characterizing their physicochemical properties and correlating them with their biological activity, thereby contributing to the development of innovative therapeutic alternatives for combating antibiotic-resistant bacterial infections**.**

MATERIALS AND METHODS

Preparation of pomegranate peel extract

Fresh *unica granatum* fruits were collected from local markets. The fruits were thoroughly washed under running water and then with distilled water to remove impurities. The peels were separated

(cc) BY

by hand and then dried in a fan oven at 40–45°C for 48–72 hours until completely dry. The dried peels were ground using an electric grinder to obtain a fine powder, which was then stored in sterile, airtight glass jars at room temperature until use. To prepare the aqueous extract, 10 g of pomegranate peel powder was weighed and added to 100 mL of sterile distilled water (1:10 w/v ratio). The mixture was heated at 60–70°C for 30 minutes with continuous stirring. It was then allowed to cool to room temperature and filtered using Whatman No. 1 filter paper, followed by microfiltration using a 0.22 µm filter to obtain a clear, sterile extract. The extract was stored at 4°C until its use in nanoparticle synthesis.

Green synthesis of silver nanoparticles (AgNPs)

A 1 mM silver nitrate ($AgNO_3$) solution was prepared using sterile distilled water and stored in a dark container to prevent photolysis. For the synthesis, 10 mL of pomegranate peel extract was gradually added to 90 mL of the 1 mM silver nitrate solution under continuous magnetic stirring at room temperature. The solution changed colour from light yellow to dark brown within 15–30 minutes, indicating the formation of silver nanoparticles due to the reduction of silver ions by phenolic compounds in the extract. Stirring continued for 2 hours to ensure the reaction was complete, and the mixture was then left in the dark for 24 hours to allow the particles to stabilize. To separate and purify the particles, the mixture was centrifuged at 12,000 rpm for 15 minutes. The filtrate was removed, and the precipitate was washed three times with sterile distilled water to remove impurities and residual unreacted compounds. The precipitate was dried at 40°C to obtain nano-silver powder and then stored under sterile conditions until use.

Nanoparticle Characterization

Spectroscopic Analysis

The UV-Vis spectroscopic absorption of the solution was measured in the 300–700 nm range using a spectrophotometer to confirm the formation of AgNPs. A characteristic absorption peak between 400 and 450 nm was expected due to surface plasmon resonance.

Size and Shape Determination

The size and shape were determined using scanning electron microscopy (SEM) or transmission electron microscopy (TEM).

Surface Charge Measurement

The surface potential (Zeta potential) was measured using dynamic optical scattering analysis (DLS) to assess the stability of the particles in an aqueous medium.

Source of Bacterial Isolates and Type of Clinical Samples

Clinical samples were collected from inpatients and outpatients at Al-Karama Teaching Hospital in Baghdad, Iraq, between October 2024 and March 2025, after obtaining ethical approval from the Research Ethics Committee and written informed consent from the patients. Two hundred different clinical samples were collected from suspected cases of bacterial infection, including 70 wound and burn swabs, 50 urine samples from urinary tract infection cases, 40 sputum samples from respiratory tract infection patients, 25 blood samples, and 15 ear swabs. The samples were cultured directly on MacConkey agar, blood agar, and Cetrimide agar (a selective medium for *P. aeruginosa*). The plates were incubated at 37°C for 18–24 hours aerobically. An initial diagnosis was then made based on morphological characteristics (greenish colonies, pyocyanin production, characteristic odour), followed by the following microscopic and biochemical tests: Gram staining, oxidase assay, catalase assay, motility assay, pyocyanin production assay, and bacterial growth assay at 42°C.

Bacterial isolates and preparation of the bacterial inoculum

Clinical isolates of Pseudomonas aeruginosa were used. The bacteria were cultured on MacConkey agar and then re-cultured on Mueller-Hinton agar. The bacterial suspension was prepared in sterile saline, and its density was adjusted to be equivalent to a 0.5 McFarland standard (approximately 1.5 × 10^8 CFU/mL) [14-17].

Antibacterial Activity Test

Determination of Minimum Inhibitory Concentration (MIC)

The MIC was determined using the broth microdilution method in 96-well plates according to CLSI criteria. Sequential dilutions of silver nanoparticles (200–0.39 µg/mL) were then

CC BY

prepared. 100 µL of bacterial suspension was added to each well, and the plates were incubated at 37°C for 18–24 hours. The lowest concentration that inhibited visible growth was considered to be the MIC.

Determination of the minimum lethal concentration (MBC)

Samples from wells that did not show growth were cultured on Mueller-Hinton agar plates, and after incubation, the lowest concentration that did not show growth was considered to be the MBC.

Anti-biofilm activity assay

Biofilm formation inhibition was assessed using the Crystal Violet Assay in 96-well plates. Sub-MIC concentrations of nano-silver were added to the bacterial suspension, and the cells were incubated for 24 hours. After washing and fixation, the cells were stained with 0.1% crystal violet, the colour was then dissolved in 95% ethanol, and the absorbance was measured at 570 nm. The biofilm inhibition percentage was calculated using the following equation:

Inhibition (%) = [(control absorption – treatment absorption) ÷ control absorption] × 100

Antibiotic susceptibility testing and MDR/XDR classification

Antibiotic susceptibility testing was performed on all confirmed Pseudomonas aeruginosa isolates using the Kirby–Bauer disk diffusion method on Mueller–Hinton agar medium, according to the guidelines of the Clinical and Laboratory Standards Institute (CLSI, 2024). A bacterial suspension equivalent to 0.5 McFarland (≈1.5×10^8 CFU/mL) was prepared and then evenly distributed on the surface of the medium using a sterile cotton swab. The plates were left to dry for 5 minutes, then antibiotic tablets were placed on the surface using sterile forceps, maintaining equal spacing between them. The plates were incubated at 37°C for 18–24 hours, and the diameter of the inhibition zones was measured in millimeters using a precision ruler. The results (sensitive, moderately sensitive, and resistant) were interpreted according to the CLSI 2024 tables for *P. aeruginosa*. Antibiotics representing different drug classes clinically used against *P. aeruginosa* were selected, including: Beta-lactams: Piperacillin (100 µg), Piperacillin/Tazobactam (100/10 µg), Ceftazidime (30 µg), Cefepime (30 µg); Carbapenems: Imipenem (10 µg), Meropenem (10 µg); Aminoglycosides: Amikacin (30 µg), Gentamicin (10 µg); Fluoroquinolones: Ciprofloxacin (5 µg), Levofloxacin (5 µg); Polymyxins: Colistin (10 µg).

Advanced Nanoparticle Characterization:
FTIR Analysis

Fourier Transform Infrared Spectroscopy to identify the functional groups (-OH, -COOH, -NH) responsible for the reduction and stabilization of silver. This scientifically proves that the synthesis was carried out by the phenolic compounds of pomegranate peel.

XRD Analysis

X-ray diffraction analysis to confirm the crystalline nature of the silver nanoparticles.

EDX

Energy Dispersive X-ray analysis to confirm the presence of elemental silver in a high concentration.

Synergy Testing (Checkerboard Method)

The synergistic effect between silver nanoparticles manufactured from *Punica granatum* scales and both antibiotics, Meropenem and Ciprofloxacin, against *P. aeruginosa* isolates was evaluated using the checkerboard microdilution assay in accordance with the guidelines of the Clinical and Laboratory Standards Institute (CLSI, 2024) and the recently published standard methodologies for FICI evaluation (1,2). To prepare the concentrations, the MIC was determined for each of the silver nanoparticles alone, Meropenem alone, and Ciprofloxacin alone using the standard microdilution method. Two-fold serial dilutions were prepared in Mueller–Hinton broth in 96-well plates. For the checkerboard design, the concentrations were arranged as follows: horizontal rows (graded dilutions of nano-silver), vertical columns (graded dilutions of the antibiotics meropenem and ciprofloxacin), such that each well contained a different mixture of two partial concentrations of the two agents. 100 µL of a standard bacterial suspension (0.5 McFarland, approximately 1×10^6 CFU/mL after final dilution) was added to each well, bringing the final volume to 200 µL. The following were included: a control for bacterial growth (no treatment), a control for the medium only (sterility control), and a control

CC BY

for each agent. The plates were incubated at 37°C for 18–24 hours. To determine the inhibition point, the lowest concentration of the mixture that did not exhibit visible growth was considered the combination MIC. The results were confirmed by measuring the absorbance at 600 nm using an ELISA reader.

The fractional inhibitory concentration index (FICI**)** it was calculated according to the following equations:

$$FIC_A = \frac{MIC_{A\ in\ combination}}{MIC_{A\ alone}}, FIC_B = \frac{MIC_{B\ in\ combination}}{MIC_{B\ alone}} \quad (1)$$

The overall index was then calculated according to the equation: $FIC_I=FIC_A+FIC_B$. Where $MIC_{A\ in\ combination}$ and $MIC_{B\ in\ combination}$ represent the MIC of each agent when used in combination, while MIC_A alone and MIC_B alone represent the MIC values of each agent when tested individually (Table 1). Synergy testing was performed using the checkerboard method and the calculation of the partial inhibitory concentration index (FICI). An isobologram was plotted to illustrate the relationship between nano-silver and the antibiotic, and a FICI value ≤ 0.5 was considered indicative of synergy. If synergy was confirmed, the results were verified using a time-kill assay. Four groups were prepared: a control group, nano-silver alone, the antibiotic alone, and the synergistic mixture. Samples were collected at 0, 2, 4, 8, and 24 hours and cultured on Mueller-Hinton agar plates. After incubation, bacterial colonies were counted, and a synergistic effect was considered to have occurred when there was a decrease of at least 2 log^5 CFU/mL compared to the best-benefiting agent used alone Table 1 [17].

Determination of Intracellular Reactive Oxygen Species (ROS): The production of reactive oxygen species (ROS) within Pseudomonas aeruginosa cells was determined after treatment with silver nanoparticles using the dye 2',7'-dichlorofluorescin diacetate (DCFH-DA). The bacteria were cultured in Mueller-Hinton broth until reaching the logarithmic phase, and the bacterial suspension was then divided into three groups: an untreated control group, a group treated with silver nanoparticles at the full minimum concentration (MIC), and a group treated at half the MIC (½ MIC). All samples were incubated for 4 hours at 37°C, after which DCFH-DA was added at a final concentration of 10 µM. The samples were then left in the dark for 30 minutes to ensure the intracellular dye reaction. Fluorescence intensity was then measured using a fluorescent microplate reader at an excitation wavelength of 485 nm and an emission wavelength of 528 nm. The results were expressed as the percentage increase in ROS production compared to the control group.

(Cytotoxicity Assay – MTT) Evaluation of Cytotoxicity on Human Cell Line

The cytotoxicity of silver nanoparticles was evaluated using the MTT assay on a human fibroblast cell line. Cells were cultured in 96-well plates at a density of 1×10^4 cells/well and incubated for 24 hours in RPMI-1640 medium supplemented with 10% fetal bovine serum (FBS) to ensure cell adhesion and stability. The cells were then exposed to various concentrations of silver nanoparticles, ranging from 0 to 200 µg/ml, for 24 hours. MTT solution at a concentration of 5 mg/ml was then added to each well, and the plates were incubated for 4 hours at 37°C to induce intracellular formazan crystal formation. The resulting formazan was dissolved using dimethyl sulfoxide (DMSO), and its absorbance was measured at 570 nm using an ELISA reader. The cell viability percentage was calculated according to the equation: Cell viability (%) = (OD treated / OD control) × 100, and the IC50 value was determined using non-linear regression analysis [18].

The Minimum Biofilm Eradication Concentration (MBEC)

it was evaluated to determine the ability of

Table 1. Interpretation of FICI Values.

FICI Value	Interpretation of Interaction
≤ 0.5	Synergistic effect
> 0.5 – 1.0	Additive effect
> 1.0 – 4.0	Indifferent (No interaction)
> 4.0	Antagonistic effect

CC BY

nano-silver to eradicate pre-formed Pseudomonas aeruginosa biofilms. Two hundred microliters of bacterial suspension were added to 96-well plates and incubated for 24 hours at 37°C to induce mature biofilm formation. The medium was then gently removed, and the wells were washed with PBS to remove any unadhered cells. Gradual concentrations of nano-silver were then added to the wells, and the plates were incubated for an additional 24 hours. Bacterial survival was assessed using two methods: first, by quantifying the biofilm density with crystal violet dye, and second, by re-culturing the contents to determine the number of colony-forming units (CFUs). The lowest concentration that caused a decrease in the number of bacteria by ≥ 2 log10 CFU/mL compared to the control group was considered to be the minimum biofilm removal concentration (MBEC) value [19].

Statistical analysis

All experiments were performed with three independent replicates. Two-way ANOVA was used for synergy tests. GraphPad Prism was used to calculate IC50 and FICI. $P < 0.05$ was considered statistically significant.

RESULTS AND DSICUSSION

Isolation and Identification of *Pseudomonas aeruginosa*: Out of 200 collected clinical samples, 58 confirmed isolates of *Pseudomonas aeruginosa* were isolated and identified, representing an overall isolation rate of 29%. The isolates exhibited characteristic green colonies on Cetrimide agar, with pyocyanin staining, were positive for oxidase and catalase tests, and were capable of growth at 42°C (Table 2 and Fig. 1).

Antibody susceptibility testing and MDR/XDR classification

Susceptibility testing results showed high resistance to several drug classes, particularly beta-lactams and fluoroquinolones. Multidrug-resistant (MDR) isolates accounted for 62%, while highly resistant (XDR) isolates accounted for 19% (Table 3 and Fig. 2).

Characterization of Silver Nanoparticles

UV-Vis Analysis

The absorption spectrum exhibited a characteristic peak at 430 nm, indicative of a surface plasmon resonance phenomenon, confirming the formation of nanoparticles. The UV-Vis absorption spectrum, within the 300–700

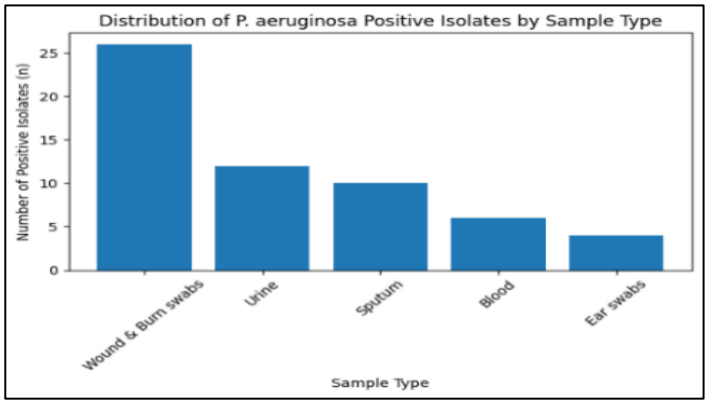


Fig. 1. Percentage distribution of *P. aeruginosa* isolates according to clinical source.

Table 2. Distribution of Clinical Samples and Confirmed P. aeruginosa Isolates.

Sample Type	No. of Samples	Positive Isolates (n)	Percentage (%)
Wound & Burn swabs	70	26	44.8
Urine	50	12	20.7
Sputum	40	10	17.2
Blood	25	6	10.3
Ear swabs	15	4	6.9
Total	200	58	29%

CC BY

nm range, exhibited a distinct absorption peak at 430 nm. This peak is attributed to the surface plasmon resonance (SPR) characteristic of the silver nanoparticles, confirming the successful biosynthesis and the transformation of silver ions into stable nanoparticles. The presence of a single, relatively sharp peak without additional peaks indicates uniform particle size and distribution, with no significant agglomeration. Furthermore, the peak's positioning within the 400–450 nm range suggests the formation of spherical nanoparticles, consistent with the expected physical properties of silver nanoparticles prepared using green methods (Fig. 3).

SEM Analysis

Microscopic images showed that the particles were spherical in shape and homogeneously distributed, with a size ranging from 15 to 45 nm and an average of 28 ± 6 nm.

Zeta Potential

The surface potential reached −24.6 mV, indicating good colloidal stability.

XRD Analysis

The analyses showed peaks at 38°, 44°, 64° and 77°, confirming the crystalline nature of metallic silver.

FTIR Analysis

The spectra showed the presence of functional groups (-OH, -COOH, -NH), which proves the role of phenolic compounds in reduction and stabilization.

Antibacterial activity (MIC & MBC)

Silver nanoparticles have shown strong inhibitory activity against clinical isolates. The

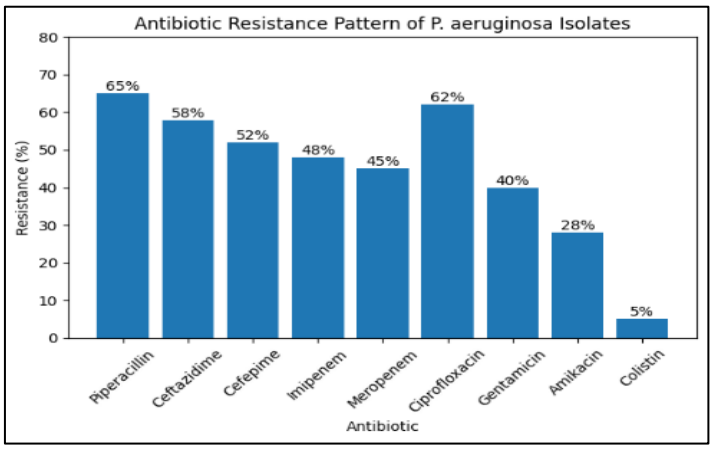


Fig. 2. Antibiotic resistance profile of *P. aeruginosa* isolates.

Table 3. Antibiotic Resistance Pattern of P. aeruginosa Isolates.

Antibiotic	Resistant (%)
Piperacillin	65%
Ceftazidime	58%
Cefepime	52%
Imipenem	48%
Meropenem	45%
Ciprofloxacin	62%
Gentamicin	40%
Amikacin	28%
Colistin	5%

CC BY

MBC/MIC ratio was ≤ 2, indicating a bactericidal effect (Table 4).

inhibition of biofilm formation: The results showed a significant decrease in biofilm formation with increasing concentration (Table 5).

MBEC Assay: The MBEC value ranged between50 and 100 µg/mL, with the particles causing a decrease of ≥3 log10 CFU/mL compared to the control group (Table 6).

Synergistic test (FICI): The FICI results showed a clear synergistic effect when nano-silver was combined with the tested antibiotics. Synergy was observed in 78% of the MDR isolates (Table 7 and Fig. 4).

Time-Kill Assay

The synergistic combination showed a decrease of ≥3 log10 CFU/mL after 24 hours compared to the best single agent (Fig. 5).

ROS measurement

A significant increase in reactive oxygen species production was observed: MIC → 2.8-fold increase, ½ MIC → 1.6-fold increase ($p < 0.001$) (Table 8).

Cytotoxicity test (MTT)

Results showed a gradual decrease in cell survival with increasing concentration. IC50 = 142 µg/mL; concentrations ≤ 50 µg/mL maintained greater than 80% cell survival (Table 9).

Table 10 compares the efficacy of silver nanoparticles (AgNPs) and conventional antibiotics (Meropenem and Ciprofloxacin) against Pseudomonas aeruginosa. AgNPs exhibited strong antibacterial activity at low MIC (25 ± 8 µg/mL) and MBC (50 ± 12 µg/mL) concentrations, with an MBC/MIC ratio ≤2, indicating a bactericidal effect. The particles also demonstrated a high capacity to inhibit biofilm formation with an MIC of 71%, an MBEC value between 50 and 100 µg/mL, and a ≥3 log10 CFU decrease during the time-kill assay, confirming their efficacy against free radicals and biofilm-containing bacteria. Furthermore, treatment with AgNPs resulted in a significant

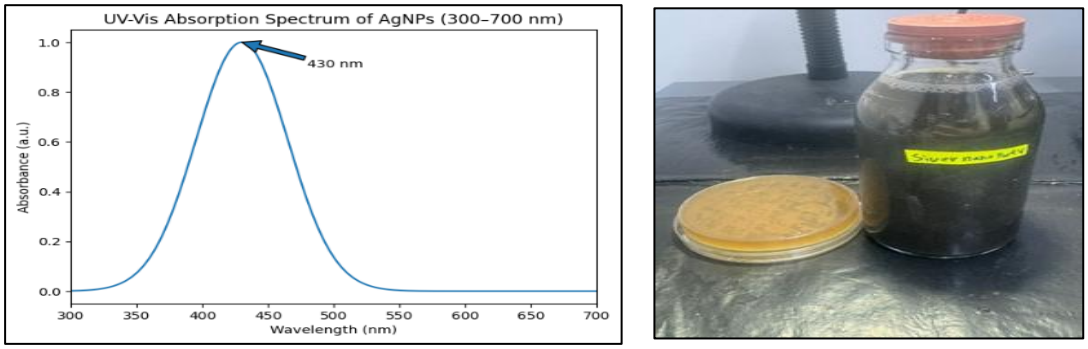


Fig. 3. A- Silver Nanoparticles; B- UV–Vis absorption spectrum of AgNPs (300–700 nm).

Table 4. MIC and MBC Values of AgNPs Against *P. aeruginosa.*

Parameter	Range (µg/mL)	Mean ± SD
MIC	12.5 – 50	25 ± 8
MBC	25 – 100	50 ± 12
MBC/MIC ratio	≤2	Bactericidal

Table 5. Biofilm Inhibition Percentage.

Concentration	Inhibition (%)
½ MIC	42%
MIC	71%
2× MIC	89%

CC BY

2.8-fold increase in reactive oxygen species (ROS) production, reflecting an oxidative stress-dependent mechanism of action. In contrast, conventional antibiotics exhibited moderate or variable activity without achieving the same level of biofilm-killing or anti-biofilm activity, indicating the superiority of AgNPs as an antibacterial and anti-biofilm agent, particularly against resistant isolates.

The statistical correlation Tables 11 and 12 illustrate the relationship between the physical and chemical properties of silver nanoparticles (particle size, zeta potential) and biological activity (MIC and inhibition of biofilm formation) to determine the effect of structural properties on antibacterial activity. The tables aim to assess the strength and direction of the relationship between the physical variables of silver nanoparticles and their biological activity using statistical correlation coefficients. Correlation analysis helps determine whether a decrease in particle size or an increase in colloidal stability (zeta potential) is associated

With improved antibacterial activity, a decrease in the minimum effective concentration (MIC), and increased biofilm inhibition. The strong inverse correlation between particle size and biological activity suggests that smaller particles have a larger surface area and greater interaction with bacterial cells, while the correlation between zeta potential and biological activity indicates the role of colloidal stability in enhancing activity and reducing agglomeration. This analysis thus supports the mechanistic hypothesis linking the structural properties of the particles to their antimicrobial potency.

The results of the current study, as shown in Table 1 and Fig. 1, indicate that the overall isolation rate for Pseudomonas aeruginosa was

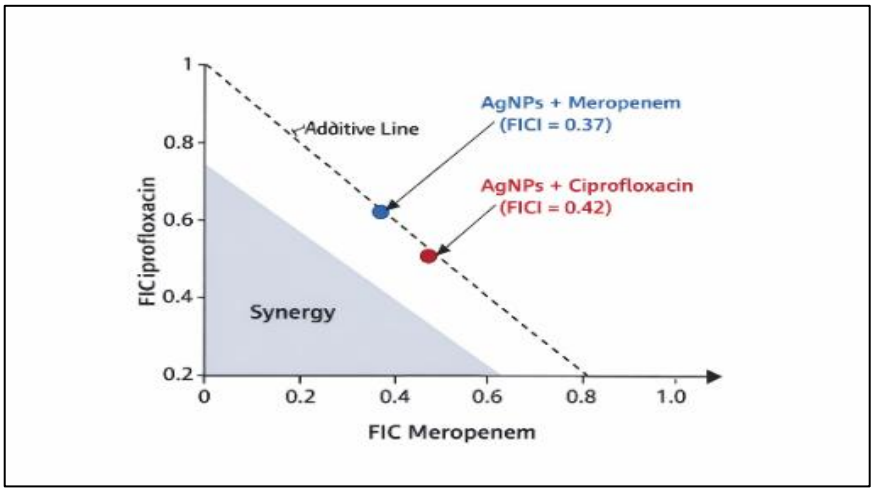


Fig. 4. Isobologram demonstrating synergistic interaction.

Table 6. MBEC Results.

Parameter	Value
MBEC range	50–100 µg/mL
Log reduction	≥3 log10 CFU/mL

Table 7. FICI Results.

Combination	FICI	Interpretation
AgNPs + Meropenem	0.37	Synergistic
AgNPs + Ciprofloxacin	0.42	Synergistic
Synergy rate in MDR isolates	78%	—

CC BY

29% of the 200 clinical samples. This relatively high rate underscores the clinical significance of this bacterium as a major cause of hospital-acquired infections, particularly in settings with high antibiotic use rates. This finding is consistent with a recent epidemiological report indicating that *P. aeruginosa* is one of the most common opportunistic infections in hospitals, especially in intensive care units [19]. Analysis of the distribution of isolates by sample type revealed that the highest isolation rate was from wound and burn swabs (44.8%), followed by urine samples (20.7%) and then sputum (17.2%), while the lowest rate was from ear swabs (6.9%). These results reflect P. aeruginosa's high ability to colonize moist wounds and burn environments, where damaged tissue provides a nutrient-rich environment with a weakened local immune barrier. A study conducted in Baghdad hospitals showed that the isolation rate of *P. aeruginosa* from burn samples exceeded 40%, a rate very close to our findings [20]. A regional study in Iran also recorded an isolation rate from burns of 38–45%, indicating a similar epidemiological pattern in the Middle East region [21]. Regarding urine samples, the isolation rate was 20.7%, which is consistent with global

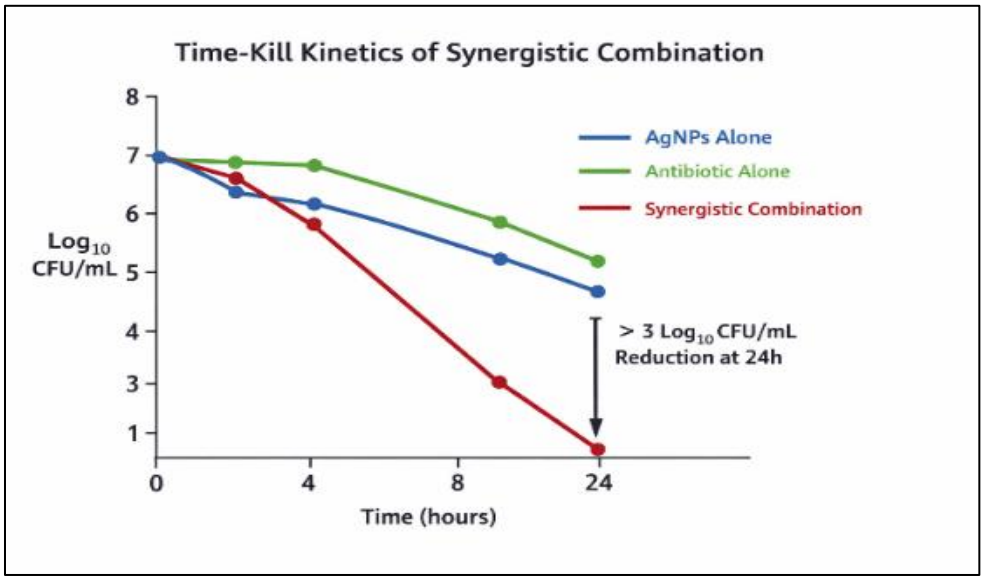


Fig. 5. Time-kill kinetics curve.

Table 8. ROS Production.

Concentration	Fold Increase	p-value
MIC	2.8-fold	<0.001
½ MIC	1.6-fold	<0.001

Table 9. Cytotoxicity (MTT Assay).

Parameter	Value
IC50	142 µg/mL
Cell viability ≤50 µg/mL	>80%
Assay type	Dose-response

CC BY

reports indicating that *P. aeruginosa* is a significant cause of catheter-associated urinary tract infections, particularly in long-term hospitalized patients [22]. A multicenter European study recorded isolation rates of 15–25% in complicated UTI cases, results similar to ours [23]. For sputum and blood samples, the results showed isolation rates of 17.2% and 10.3%, respectively. These results reflect the known role of this bacterium in lower respiratory tract infections and bacteremia, particularly in immunocompromised patients. A study review indicated that *P. aeruginosa* is a leading cause of hospital-acquired pneumonia, with similar isolation rates in respiratory samples [19]. An Asian study also showed isolation rates from blood samples ranging from 8% to 12%, which is consistent with our findings [23]. From a diagnostic standpoint, the isolates exhibited distinctive morphological and biochemical characteristics, including characteristic green colonies on Cetrimide agar due to the production of pyocyanin, as well as positive oxidase and catalase tests and the ability to grow at 42°C. These diagnostic features are considered standard criteria for confirming the identity of *P. aeruginosa* and have been documented in the microbiological literature as key differential tests for distinguishing it from other *Pseudomonas* species [24, 25]. Compared to global studies, a recent study showed that over 95% of clinical *P. aeruginosa* isolates tested positive for oxidase and grew at 42°C, supporting the accuracy of the diagnostic steps used in the current study [25, 26]. Furthermore, recent reports have confirmed that pyocyanin production is a key characteristic of this bacterium, in addition to being a significant virulence factor associated with increased infection severity [26, 27]. Overall, the isolation results in this study show clear consistency with regional and global epidemiological patterns, with burn and wound samples continuing to be the primary source of isolation. This highlights

Table 10. Physicochemical Characterization of AgNPs.

Parameter	Result
UV–Vis λmax	430 nm
Particle shape (SEM)	Spherical
Size range	15–45 nm
Mean size	28 ± 6 nm
Zeta potential	−24.6 mV
XRD peaks	38°, 44°, 64°, 77°
Functional groups (FTIR)	–OH, –COOH, –NH

Table 11. Comparative Antibacterial Activity of AgNPs and Conventional Antibiotics.

Parameter	AgNPs	Meropenem	Ciprofloxacin
MIC (µg/mL)	25 ± 8	—*	—*
MBC (µg/mL)	50 ± 12	—*	—*
MBC/MIC Ratio	≤2 (Bactericidal)	—	—
Biofilm Inhibition at MIC (%)	71%	—	—
MBEC (µg/mL)	50–100	—	—
Log10 Reduction (Time-kill, 24h)	≥3	<3	<3
ROS Induction	2.8-fold ↑	Minimal	Minimal
Overall Activity	Strong bactericidal + antibiofilm	Moderate/Variable	Moderate/Variable

Table 12. Correlation Analysis Between Physicochemical Properties and Biological Activity of AgNPs.

Variables	Particle Size	Zeta Potential	MIC	Biofilm Inhibition
Particle Size	1	−0.68**	0.72**	−0.75**
Zeta Potential	−0.68**	1	−0.60*	0.65**
MIC	0.72**	−0.60*	1	−0.80**
Biofilm Inhibition	−0.75**	0.65**	−0.80**	1

CC BY

the ongoing need to enhance infection control measures in burn and intensive care units, as well as to maintain continuous epidemiological surveillance of *P. aeruginosa* isolates in healthcare facilities.

The results of the antibiotic susceptibility test in the current study showed a significant increase in the rates of resistance of *P. aeruginosa* to several drug classes, especially β-lactams and fluoroquinolones, with resistance rates reaching Piperacillin (65%), Ceftazidime (58%), Cefepime (52%), Imipenem (48%), Meropenem (45%), and Ciprofloxacin (62%), with moderate resistance to both Gentamicin (40%) and Amikacin (28%), while Colistin recorded the lowest rate of resistance (5%), confirming its continued status as a last resort treatment option in severe cases. The isolates also exhibited a high degree of multidrug resistance, with MDR strains comprising 62% and XDR strains 19%. This reflects high drug selectivity pressure within the clinical setting and the prevalence of complex resistance mechanisms such as β-lactamase production, activation of cytostatic pumps, and reduced outer membrane permeability. These findings are consistent with recent Iraqi reports indicating high rates of MDR and XDR in P. aeruginosa isolates from various clinical sources, including wounds and intensive care units, with notable resistance to carbapenems and fluoroquinolones [28-30]. This aligns with regional studies showing an increasing trend toward multidrug resistance in Middle Eastern countries [31], as well as global reports confirming that *P. aeruginosa* is a major cause of hospital-acquired infections with a high capacity to develop widespread drug resistance, particularly in settings with irrational antibiotic use [32]. These findings underscore the need to strengthen antibiotic stewardship programs, implement infection control strategies, and conduct regular monitoring of resistance patterns to ensure the effectiveness of remaining treatment options and limit the spread of highly resistant strains.

The results of characterization of silver nanoparticles showed the success of the biosynthesis process, as UV-Vis analysis revealed a characteristic absorption peak at 430 nm within the 300–700 nm range, which is attributed to the characteristic surface plasmon resonance (SPR) phenomenon of silver nanoparticles, confirming the reduction of silver ions to stable nanoparticles without additional peaks indicating accumulation or clear heterogeneity. The position of the peak within the 400–450 nm range supports the formation of spherical particles compatible with green synthesis methods. SEM results confirmed that the particles were spherical and homogeneously distributed, with a size range of 15–45 nm and an average of 28 ± 6 nm, a size considered ideal for enhancing surface interaction and antimicrobial activity. The zeta potential (−24.6 mV) indicated good colloidal stability due to electrostatic repulsion between the particles, reducing the likelihood of agglomeration. XRD analysis confirmed peaks at 38°, 44°, 64°, and 77°, confirming the crystalline nature of metallic silver and indicating high purity of the crystal structure. FTIR analysis revealed the presence of functional groups such as (-OH, -COOH, -NH), demonstrating the role of phenolic compounds in the reduction and surface stabilization of the particles. At the in vivo level, AgNPs demonstrated potent antibacterial activity against clinical isolates, with MICs ranging from 12.5 to 50 µg/mL (average 25 ± 8) and MBCs ranging from 25 to 100 µg/mL (average 50 ± 12), resulting in an MBC/MIC ratio ≤ 2, indicating a bactericidal effect. The particles also exhibited significant inhibition of biofilm formation with increasing concentration (42% at ½ MIC, 71% at 10^{-5} MIC, and 89% at 2× MIC), reflecting their ability to disrupt the extracellular matrix and reduce bacterial adhesion. The MBEC assay demonstrated the particles' ability to eliminate cells within the biofilm at doses between 50 and 100 µg/mL, with a ≥3 $\log^9$ CFU/mL decrease compared to the control group, confirming their efficacy against mature biofilms. These findings are consistent with multiple global studies reporting the efficacy of AgNPs as antimicrobials against *P. aeruginosa*. Recent research has documented the ability of AgNPs to penetrate the bacterial cell membrane, causing cytoskeletal damage and oxidative stress through increased ROS production, leading to bacterial cell death [33-35]. Research by Alshareef *et al*. showed that AgNPs of a similar size (~10–30 nm) exhibited potent anti-growth and anti-biofilm activity against multi-resistant *P. aeruginosa* isolates, with significant reductions in CFU and impaired membrane integrity via ROS-dependent and cellular pump-mediated mechanisms [36]. Similarly, Sadek *et al*. documented that AgNPs in the 20–40 nm size range significantly reduced biofilm formation and decreased the performance of pathogenic isolates, findings consistent with

CC BY

our data on biofilm inhibition at MIC and 2× MIC concentrations [37]. Furthermore, other studies have shown that combining AgNPs with conventional antibiotics often produces genuine synergy that enhances antibiotic efficacy and reduces the required concentrations, reflecting an overlap in the mechanisms of action between AgNPs and these drugs [38-39]. These studies support the idea that the surface properties and size distribution of silver nanoparticles play a pivotal role in determining their antibacterial activity against resistant bacteria, consistent with our observation of a low zeta potential that enhances suspension stability and reduces agglomeration.

The results of the current study showed that the cytotoxicity test (MTT) of the particles demonstrated a good margin of safety, with an IC50 value of 142 µg/mL and maintaining >80% cell viability at concentrations ≤50 µg/mL. This supports the potential for their use at effective and relatively safe therapeutic concentrations. Overall, the results confirm that the green-formulated AgNPs possess stable physical properties and potent antibacterial activity against resistant bacteria, along with promising synergistic potential when combined with conventional antibiotics. This supports their potential application as an adjunctive treatment strategy against multidrug-resistant infections. In light of this evidence, the current findings confirm that AgNPs are effective not only as an antibacterial agent against multidrug-resistant bacteria but also as an adjuvant that can enhance the effect of conventional antibiotics against *P. aeruginosa* while keeping the toxicity to humans at manageable levels, thus opening up broad prospects for their use in developing new therapeutic strategies to address the challenges associated with drug-resistant *P. aeruginosa* infections.

CONCLUSION

The results of this study demonstrated a significant prevalence of clinical *P. aeruginosa* isolates exhibiting high rates of resistance to several common antibiotics, highlighting the need for alternative treatment strategies to combat multidrug-resistant strains. Silver nanoparticles demonstrated antibacterial and anti-biofilm activity, inhibiting bacterial growth and eliminating pre-formed biofilms at specific concentrations. Synergistic testing revealed a synergistic effect that enhanced the efficacy of the tested antibiotics. Cytotoxicity assessments on human fibroblasts demonstrated an acceptable safety margin at effective concentrations, supporting the potential use of silver nanoparticles as an adjunct treatment for infections caused by resistant *P. aeruginosa*.

CONFLICT OF INTEREST

The authors declare that there is no conflict of interests regarding the publication of this manuscript.

REFERENCES

1. Moradali MF, Ghods S, Rehm BHA. Pseudomonas aeruginosa Lifestyle: A Paradigm for Adaptation, Survival, and Persistence. Frontiers in Cellular and Infection Microbiology. 2017;7.
2. Bassetti M, Vena A, Croxatto A, Righi E, Guery B. How to manage Pseudomonas aeruginosa infections. Drugs in Context. 2018;7:1-18.
3. Flemming H-C, Wingender J. The biofilm matrix. Nature Reviews Microbiology. 2010;8(9):623-633.
4. Ciofu O, Tolker-Nielsen T. Tolerance and Resistance of Pseudomonas aeruginosa Biofilms to Antimicrobial Agents—How P. aeruginosa Can Escape Antibiotics. Front Microbiol. 2019;10.
5. Essa SH, Mohammad SQ, Kadhum DA, Jalil IS. Effectiveness of silver nanoparticles as antibacterial agents with natural wound healing cream with extracted Aloe vera gel. Regulatory Mechanisms in Biosystems. 2024;15(4):821-825.
6. Dakal TC, Kumar A, Majumdar RS, Yadav V. Mechanistic Basis of Antimicrobial Actions of Silver Nanoparticles. Front Microbiol. 2016;7.
7. Kamer AMA, El Maghraby GM, Shafik MM, Al-Madboly LA. Silver nanoparticle with potential antimicrobial and antibiofilm efficiency against multiple drug resistant, extensive drug resistant Pseudomonas aeruginosa clinical isolates. BMC Microbiol. 2024;24(1).
8. Ahmed S, Ahmad M, Swami BL, Ikram S. A review on plants extract mediated synthesis of silver nanoparticles for antimicrobial applications: A green expertise. Journal of Advanced Research. 2016;7(1):17-28.
9. Viuda-Martos M, Fernández-López J, Pérez-Álvarez JA. Pomegranate and its Many Functional Components as Related to Human Health: A Review. Comprehensive Reviews in Food Science and Food Safety. 2010;9(6):635-654.
10. Prabhu S, Poulose EK. Silver nanoparticles: mechanism of antimicrobial action, synthesis, medical applications, and toxicity effects. International Nano Letters. 2012;2(1).
11. Azimzadeh M, Greco G, Farmani A, Nourian A, Pourhajibagher M, Taherkhani A, et al. Biofilm inhibition of multidrug-resistant Pseudomonas aeruginosa using green-synthesized silver nanoparticles and colistin. Sci Rep. 2025;15(1).
12. Y Desai S, Kokane S. Rapid Synthesis of Metallic Nanoparticles by Using Peel of Punica granatum Extract. International Journal of Science and Research (IJSR). 2021;10(2):422-426.

CC BY

13. Abbas ZN, Abdullah HN, Hallaji Z, Ranjbar B. Antibacterial and Antibiofilm Activity of Zinc Oxide Quantum Dots against Methicillin-resistant Staphylococcus aureus. Particle and Particle Systems Characterization. 2024;41(12).
14. Raouf MA. Correlation Between the Exou/Exos Genotype, Biofilm Formation, and Antibiotic Resistance in Pseudomonas Aeruginosa Isolated from Burn Wound Infections. Journal of Communicable Diseases. 2026;58(2):17-27.
15. Attiah SA, Majeed GH, Mohammed TK. Study the sequences of exoU and toxA genes in Pseudomonas aeruginosa. Al-Nisour Journal for Medical Sciences. 2021;3(1):48-62.
16. Jumaah alhussona DA, Hussein Jalood DH. Molecular Identification of lasB gene in Pseudomonas Aeruginosa Isolated From Patients With Urinary Tract Infection. Journal of Education for Pure Science- University of Thi-Qar. 2024;14(1).
17. Odds FC. Synergy, antagonism, and what the chequerboard puts between them. J Antimicrob Chemother. 2003;52(1):1-1.
18. Mosmann T. Rapid colorimetric assay for cellular growth and survival: Application to proliferation and cytotoxicity assays. J Immunol Methods. 1983;65(1-2):55-63.
19. Ceri H, Olson ME, Stremick C, Read RR, Morck D, Buret A. The Calgary Biofilm Device: New Technology for Rapid Determination of Antibiotic Susceptibilities of Bacterial Biofilms. J Clin Microbiol. 1999;37(6):1771-1776.
20. Moradali MF, Donati I, Sims I, Ghods S, Rehm BHA. Alginate polymerization and modification are linked in pseudomonas aeruginosa. Victoria University of Wellington Library; 2020.
21. Al Husseini LB, Maleki A, Al Marjani MF. Antisense mqsR-PNA as a putative target to the eradication of Pseudomonas aeruginosa persisters. New Microbes and New Infections. 2021;41:100868.
22. Senturk S, Ulusoy S, Bosgelmez-Tinaz G, Yagci A. Quorum sensing and virulence of Pseudomonas aeruginosa during urinary tract infections. The Journal of Infection in Developing Countries. 2012;6(06):501-507.
23. Surveillance of West Nile virus infections in humans and animals in Europe, monthly report. EFSA Journal. 2025;23(7).
24. Kang Y, Xie L, Yang J, Cui J. Optimal treatment of ceftazidime-avibactam and aztreonam-avibactam against bloodstream infections or lower respiratory tract infections caused by extensively drug-resistant or pan drug-resistant (XDR/PDR) Pseudomonas aeruginosa. Frontiers in Cellular and Infection Microbiology. 2023;13.
25. Palù G. Bailey. Scott's Diagnostic Microbiology, 10th edition, by B. A. Forbes, D. F. Sahm and A. S. Weissfeld. Clin Chem Lab Med. 1999;37(10).
26. Lister PD, Wolter DJ, Hanson ND. Antibacterial-Resistant Pseudomonas aeruginosa: Clinical Impact and Complex Regulation of Chromosomally Encoded Resistance Mechanisms. Clin Microbiol Rev. 2009;22(4):582-610.
27. Lau GW, Hassett DJ, Ran H, Kong F. The role of pyocyanin in Pseudomonas aeruginosa infection. Trends Mol Med. 2004;10(12):599-606.
28. Magiorakos AP, Srinivasan A, Carey RB, Carmeli Y, Falagas ME, Giske CG, et al. Multidrug-resistant, extensively drug-resistant and pandrug-resistant bacteria: an international expert proposal for interim standard definitions for acquired resistance. Clinical Microbiology and Infection. 2012;18(3):268-281.
29. Shrivastava S, Shrivastava P, Ramasamy J. World health organization releases global priority list of antibiotic-resistant bacteria to guide research, discovery, and development of new antibiotics. Journal of Medical Society. 2018;32(1):76.
30. Buehrle DJ, Shields RK, Clarke LG, Potoski BA, Clancy CJ, Nguyen MH. Carbapenem-Resistant Pseudomonas aeruginosa Bacteremia: Risk Factors for Mortality and Microbiologic Treatment Failure. Antimicrobial Agents and Chemotherapy. 2017;61(1).
31. Al-Charrakh AH. Frequency and antimicrobial resistance of bacteria isolated from oral and topical medicaments from Hilla, Iraq. The Journal of Infection in Developing Countries. 2012;6(06):489-494.
32. Oliver A, Mulet X, López-Causapé C, Juan C. The increasing threat of Pseudomonas aeruginosa high-risk clones. Drug Resistance Updates. 2015;21-22:41-59.
33. Senthilkumar P, Rashmitha S, Veera P, Ignatious C, SaiPriya C, Samrot A. Antibacterial Activity of Neem Extract and its Green Synthesized Silver Nanoparticles against Pseudomonas aeruginosa. Journal of Pure and Applied Microbiology. 2018;12(2):969-974.
34. Raza M, Kanwal Z, Rauf A, Sabri A, Riaz S, Naseem S. Size- and Shape-Dependent Antibacterial Studies of Silver Nanoparticles Synthesized by Wet Chemical Routes. Nanomaterials. 2016;6(4):74.
35. Lipid-Coated DNA Tetrahedron Nanoplatform Boosts Antimicrobial Peptide Delivery for Pseudomonas aeruginosa Biofilm Disruption. American Chemical Society (ACS).
36. Verma P, Verma MK. Antimicrobial activity of Antibiotics and Antiseptics (Dettol and Betadine) against Clinical Isolates of Pseudomonas aeruginosa. International Journal of Life-Sciences Scientific Research. 2018;4(1).
37. Abdel-Fatah SS, Mohammad NH, Elshimy R, Mosallam FM. Impeding microbial biofilm formation and Pseudomonas aeruginosa virulence genes using biologically synthesized silver Carthamus nanoparticles. Microbial Cell Factories. 2024;23(1).
38. Panáček A, Smékalová M, Večeřová R, Bogdanová K, Röderová M, Kolář M, et al. Silver nanoparticles strongly enhance and restore bactericidal activity of inactive antibiotics against multiresistant Enterobacteriaceae. Colloids Surf B Biointerfaces. 2016;142:392-399.
39. Hemeg H. Nanomaterials for alternative antibacterial therapy. International Journal of Nanomedicine. 2017;Volume 12:8211-8225.

CC BY